Supercontinuum generation from 1.35 to 1.7 mu m by nanosecond pumping near the second zero-dispersion wavelength of a microstructured fiber

A. Boucon, D. Alasia, J.C. Beugnot, S. Mélin, S. Lempereur, A. Fleureau, H. Maillotte, J.M. Dudley, T. Sylvestre

Supercontinuum Generation From 1.35 to 1.7μm by Nanosecond Pumping Near the Second Zero-Dispersion Wavelength of a Microstructured Fiber

A. Boucon, D. Alasia, J. C. Beugnot, G. Mélin, S. Lempereur, A. Fleureau, H. Maillotte, J. M. Dudley, *Senior Member, IEEE*, and T. Sylvestre

***Abstract*—We experimentally study a new regime for supercontinuum (SC) generation in the nanosecond pulsed regime using a microstructured optical fiber with two zero-dispersion wavelengths (ZDWs). Pumping at 1535 nm around the second ZDW yields a nearly flat SC over 1350–1700 nm. The interplay between the effects of modulation instability and stimulated Raman scattering are described through simple phase-matching relations.**

***Index Terms*—Nonlinear optics, optical fiber, supercontinuum (SC) generation.**

I. Introduction

BROADBAND optical supercontinuum (SC) sources continue to attract intense research interest because of their numerous important applications in domains ranging from optical frequency metrology to biophotonic imaging [1]. Recent years have seen particular focus on SC generation in microstructured optical fiber where enhanced confinement and the possibility to engineer the zero-dispersion wavelength (ZDW) into spectral regions accessible by a wide variety of different pump sources have led to a number of impressive studies over a wide range of wavelengths [2], [3]. Although initial studies of SC generation used fibers with only one ZDW typically in the visible or near-infrared wavelength range, there has been increasing interest in the properties of SC generation in microstructured fiber presenting two ZDWs [4]–[8]. In contrast to these previous studies where femtosecond pulse propagation and/or soliton dynamics were the dominant spectral broadening mechanisms, our purpose here is to report a detailed experimental study of SC generation around the second ZDW of a microstructured fiber using a nanosecond pulsed source at 1535 nm. SC generation using longer pulses in the quasi-continuous-wave dynamical regime exhibits a number of specific features, and we consider in particular the interplay between the effects of modulation instability (MI) and stimulated Raman scattering (SRS) and describe experimental results showing spectral broadening from 1350 to 1700 nm. Cascaded anti-Stokes Raman generation due to phase-matching allowed by the group-velocity dispersion is also reported.

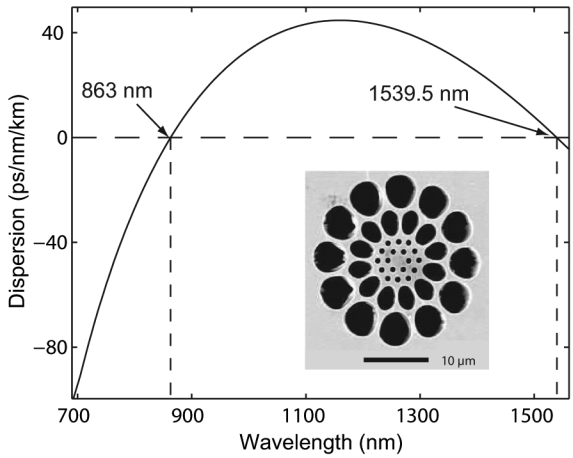

Fig. 1. Dispersion curve for the fundamental mode exhibiting two ZDWs at 863 and 1539.5 nm, respectively. The inner plot shows a scanning electron microscope image of the fiber cross section.

II. Experimental Setup

The pump source used in our experiments was a compact Q-switched microchip laser (Cobolt) emitting at 1535 nm with a repetition rate of 3.3 kHz, average power of 17 mW, and a nominal pulse length of 3.1 ns. The laser beam was injected into the microstructured fiber by means of a 20 $\times$ microscope objective and the spectra were recorded at the output of the fiber using an optical spectrum analyzer (OSA). The fiber was spliced at both ends to standard single-mode fiber (SMF28) pigtails, leading to a maximum coupling efficiency of about 30%. The MI and SC characteristics were conveniently examined as a function of peak power by adjusting the coupling efficiency. The microstructured fiber used in our experiments had a geometry consisting of four rings of holes, with different diameters, as shown in the inner picture in Fig. 1. The fiber length was 38 m. The chromatic dispersion properties are primarily determined by the geometry of the two internal rows based on a triangular lattice placed around the core [9]. The effective area is $A_{\text{eff}} = 5\ \mu\text{m}^2$ and the nonlinear coefficient at the pump wavelength is $\gamma = 2\pi n_2/(\lambda A_{\text{eff}}) = 20.5\ \text{W}^{-1} \cdot \text{km}^{-1}$, where $n_2 = 2.5 \times 10^{-20}\ \text{m}^2\text{W}^{-1}$. The group velocity dispersion of the

Manuscript received November 26, 2007; revised February 12, 2008. This work was supported by the Conseil Général de Franche-Comté and by the Ministère déléguéà la Recherche.

A. Boucon, D. Alasia, J. C. Beugnot, H. Maillotte, J. M. Dudley, and T. Sylvestre are with the Institut FEMTO-ST, Département d'Optique P.M. Duffieux, CNRS-Université de Franche-Comté, UMR 6174, 25030 Besançon, France (e-mail: anne.boucon@univ-fcomte.fr; thibaut.sylvestre@univ-fcomte.fr).

G. Mélin, S. Lempereur, and A. Fleureau are with the DRAKA, 91460 Marcoussis, France.

Digital Object Identifier 10.1109/LPT.2008.921824

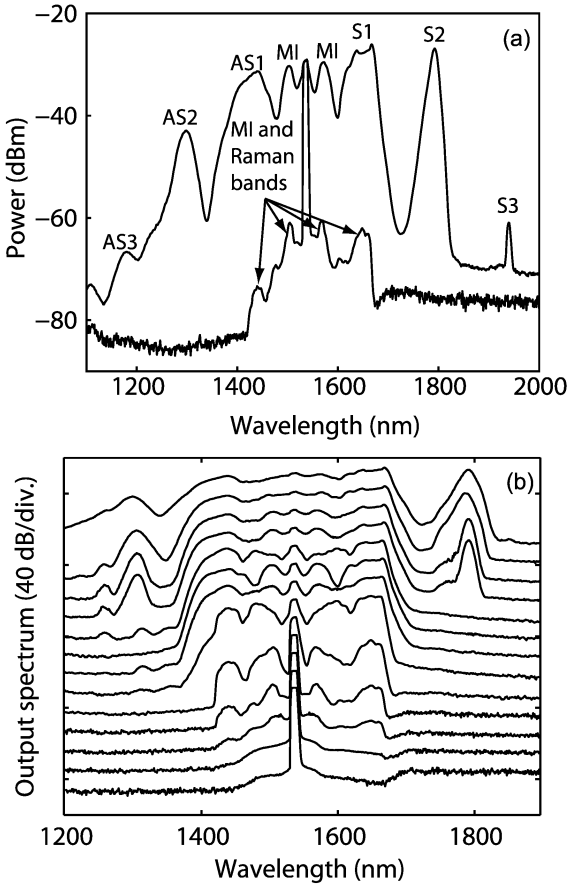

Fig. 2. (a) Output spectra measured at the output end of the fiber for two output mean pump powers of 200 μW and 1 mW, respectively. S and AS bands denote, respectively, by the multiple Stokes and anti-Stokes Raman components. MI denotes the MI sidebands. (b) Spectra recorded at the end of the fiber for increasing pump powers from 50 μW to 1.3 mW.

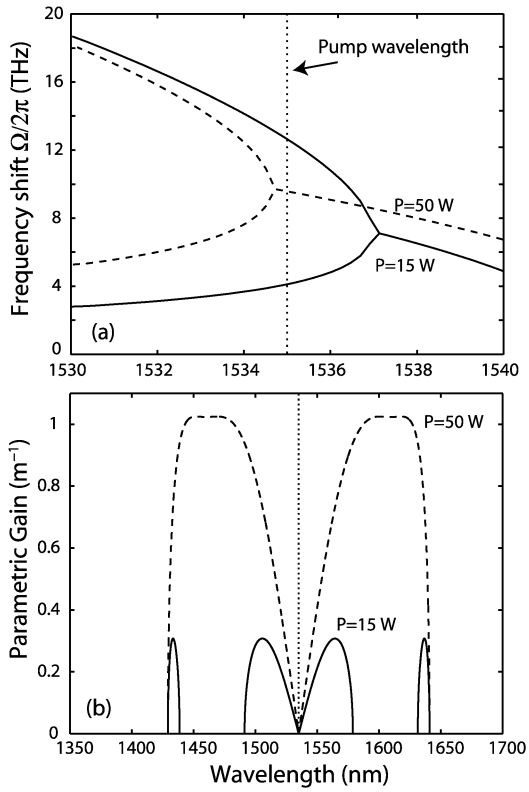

Fig. 3. (a) Frequency shift between pump and MI sidebands $\Omega/2\pi$ in function of the pump wavelength at low (solid line) and high pump power (dashed line). (b) Corresponding parametric gain spectra.

fundamental mode has been calculated using the MODE Solutions numerical tool developed by Lumerical, and is shown in Fig. 1. We clearly see the existence of two ZDWs located, respectively, at 863 and 1539.5 nm with anomalous GVD over the range 863–1539.5 nm and normal GVD elsewhere. The second-, third-, and fourth-order dispersion coefficients, calculated at the pump wavelength of 1535 nm, are $\beta_2 = -1.207$ ps$^2 \cdot$ km^{-1}, $\beta_3 = -0.315$ ps$^3 \cdot$ km^{-1}, and $\beta_4 = 0.002$ ps$^4 \cdot$ km^{-1}, respectively. Note that, at pump wavelength, the sign of the third-order dispersion (dispersion slope) is negative.

III. Experimental Results and Analysis

The spectra measured at the output end of the fiber for different increasing input powers are shown in Fig. 2. Although femtosecond pulse SC generation involves an initial (deterministic) propagation phase of higher order soliton evolution, SC generation in the nanosecond regime involves a significantly different (noise-induced) scenario [10], [11]. Specifically, the pump near the ZDW undergoes spectral broadening through MI, which is manifested, in the Fourier domain, by the clear generation of two or more sidebands symmetrically located around the pump. When pumping close to the ZDW as in our experiments, calculation of the MI sideband positions must include higher order dispersion terms according to the phase-matching relation [12]: $\kappa = \beta_2\Omega^2 + (\beta_4/12)\Omega^4 + 2\gamma P = 0$, where β_2 and β_4 are the second- and fourth-order dispersion coefficients, γ is the nonlinear coefficient of the fiber, P is the peak power, and $\Omega = \omega_{\mathrm{MI}} - \omega_P$ is the frequency shift between the pump and the instability bands.

Fig. 3(a) shows the solutions of this equation for two power levels. We can see that at a pump power of 15 W, two solutions for $|\Omega|$ are possible due to an interplay between the signs of the second- and the fourth-order coefficients. That means two closely spaced modulation bands located at each side of the pump are generated at 1501.3 and 1570.2 nm for the first solution, and at 1441 and 1642.1 nm for the second solution, as indicated in Fig. 2(a) with arrows. This situation is clearly illustrated as a solid line in Fig. 3(b) that shows the parametric or MI gain spectrum in unit length derived from the usual expression $g^2 = (\gamma P)^2 - (\kappa/2)^2$ [13]. Note that, in particular, the second solutions lie within the Stokes and anti-Stokes Raman bands. At high pump power, the dashed lines of Fig. 3(a) and (b) indicate that there is only one solution left but with a corresponding ultrabroad gain band with a wide range of phase-matched frequencies including the first-order Raman bands.

Raman scattering also plays a central role in the SC generation and manifests itself through the appearance of a Stokes band which is frequency down-shifted by approximately 13.2 THz from the pump. By copropagating with the pump, the Stokes wave can easily seed the generation of additional higher Raman orders through a cascading process [3]. We show, in Fig. 2(a), the generation of a first Raman order (S1),

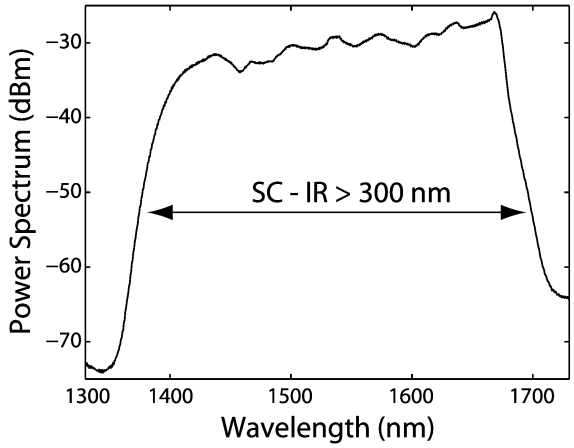

Fig. 4. SC spectrum recorded in the 1300- to 1750-nm range at the end of the fiber at maximum launched power.

strongly seeded by the MI process, and one can also notice the appearance, for sufficiently high pump power, of a second (S2) and third (S3) Raman order. Note that the latter S3 at 1930 nm appears with a small amplitude in the spectrum because of the low quantum efficiency of the OSA detector at that wavelengths. Such a Raman cascade can be clearly observed because the Stokes bands fall within the normal dispersion regime and do not undergo significant spectral broadening or soliton self-frequency shift dynamics [4], as it is generally the case when pumping near the first ZDW. Unlike the MI process, the Raman gain is anti-symmetric and spectral components of the anti-Stokes side are in principle attenuated. However, the observation of strong anti-Stokes Raman components (AS1, AS2, AS3)—as shown in Fig. 2(a)—is observed due to the coupling between SRS and parametric gain, and also indicates that four-wave mixing processes strongly contribute to the SC generation [10]. In particular, the first anti-Stokes Raman order is strongly generated by phase-matched four-wave mixing because it lies within the MI second solutions, as shown in Fig. 3(a) and (b). Although the results in Fig. 2(a) suggest our experiment demonstrates the explicit appearance of the four MI sidebands predicted in Fig. 3, the overlap of the sideband spacing with the Raman frequency shift make it difficult to unambiguously interpret the results in this way. In Fig. 2(b), we show several typical output spectra recorded for different increasing pump powers and show that the anti-Stokes components grow and broaden as far as the input power increases. The spectral broadening of all anti-Stokes Raman order can be attributed to the fact that they fall in the anomalous dispersion regime and, therefore, are modulationally unstable. Finally, the anti-Stokes bands become comparable to the Stokes components and efficiently contribute to the generation of a nearly flat 350-nm-large SC, almost entirely covering the whole telecommunication band region from E to XL. A full spectrum of SC extending from 1350 to 1700 nm is depicted in Fig. 4. The total SC output mean power was measured to 1.3 mW.

IV. Conclusion

SC generation in a microstructured optical fiber by nanosecond pumping near the second ZDW with potential telecommunication applications has been demonstrated. The specificity of pumping near the second ZDW with a negative dispersion slope makes possible the generation of an unbroadened Raman cascade up to three orders. The interplay between SRS and parametric or MI gain is responsible for the generation of anti-Stokes components that broaden and efficiently contribute to the SC generation. At high pump power, the SC covers the range 1350–1700 nm with good spectral flatness. This SC could directly find potential applications for telecommunication components testing and wavelength-division multiplexing.

References

[1] R. R. Alfano, Ed., *The Supercontinuum Laser Source*. New York: Springer, 2006.

[2] J. K. Ranka, R. S. Windeler, and A. J. Stentz, "Visible continuum generation in air-silica microstructure optical fibers with anomalous dispersion at 800 nm," *Opt. Lett.*, vol. 25, no. 1, pp. 25–27, Jan. 2000.

[3] J. M. Dudley, G. Genty, and S. Coen, "Supercontinuum generation in photonic crystal fiber," *Rev. Mod. Phys.*, vol. 78, pp. 1135–1184, Oct./Dec. 2006.

[4] D. V. Skryabin, F. Luan, J. C. Knight, and P. St. J. Russell, "Soliton self-frequency shift cancellation in photonic crystal fibers," *Science*, vol. 301, pp. 1705–1708, Sep. 19, 2003.

[5] K. M. Hilligsøe, T. V. Andersen, H. N. Paulsen, C. K. Nielsen, K. Mølmer, S. Keiding, R. Kristiansen, K. P. Hansen, and J. J. Larsen, "Supercontinuum generation in a photonic crystal fiber with two zero dispersion wavelengths," *Opt. Express*, vol. 12, no. 6, pp. 1045–1053, Mar. 2004.

[6] M.-L. V. Tse, P. Horak, F. Poletti, N. G. Broderick, J. H. Price, J. R. Hayes, and D. J. Richardson, "Supercontinuum generation at 1.06 μm in holey fibers with dispersion flattened profiles," *Opt. Express*, vol. 14, no. 10, pp. 4445–4451, 2006.

[7] M. H. Frosz, P. Falk, and O. Bang, "The role of the second zero-dispersion wavelength in generation of supercontinua and bright-bright soliton-pairs across the zero-dispersion wavelength," *Opt. Express*, vol. 13, no. 16, pp. 6181–6192, Aug. 2005.

[8] A. Mussot, M. Beaugeois, M. Bouazaoui, and T. Sylvestre, "Tailoring CW supercontinuum generation in microstructured fibers with two-zero dispersion wavelengths," *Opt. Express*, vol. 15, no. 18, p. 11553, Sep. 2007.

[9] G. Mélin, L. Provost, X. Rejeaunier, E. Bourova, A. Fleureau, S. Lempereur, and L. Gasca, "Innovative design for highly non-linear microstructured fibers," in *Eur. Conf. Opt. Commun.*, Stockholm, Sweden, Sep. 5–9, 2004, vol. 2, pp. 232–233, Paper Tu4.3.2.

[10] S. Coen, A. H. L. Chau, R. Leonhardt, J. D. Harvey, J. C. Knight, W. J. Wadsworth, and P. St. J. Russell, "Supercontinuum generation by stimulated Raman scattering and parametric four-wave mixing in photonic crystal fibers," *J. Opt. Soc. Amer. B, Opt. Phys.*, vol. 19, no. 4, pp. 753–764, Apr. 2002.

[11] J. M. Dudley, L. Provino, N. Grossard, H. Maillotte, R. Windeler, B. Eggleton, and S. Coen, "Supercontinuum generation in air-silica microstructured fibers with nanosecond and femtosecond pulse pumping," *J. Opt. Soc. Amer. B, Opt. Phys.*, vol. 19, no. 4, pp. 765–770, Apr. 2002.

[12] J. D. Harvey, R. Leonhardt, S. Coen, G. K. L. Wong, J. C. Knight, W. J. Wadsworth, and P. S. J. Russell, "Scalar modulation instability in the normal dispersion regime by use of a photonic crystal fiber," *Opt. Lett.*, vol. 28, no. 22, pp. 2225–2227, Nov. 2003.

[13] G. P. Agrawal, "Nonlinear Fiber Optics," in *Optics and Photonics*, 3rd ed. San Diego, CA: Academic, 2001.